

This is the accepted manuscript made available via CHORUS. The article has been published as:

Non-Hermitian quantum annealing in the ferromagnetic Ising model

Alexander I. Nesterov, Juan Carlos Beas Zepeda, and Gennady P. Berman

Phys. Rev. A **87**, 042332 — Published 25 April 2013

DOI: [10.1103/PhysRevA.87.042332](https://doi.org/10.1103/PhysRevA.87.042332)

Non-Hermitian Quantum Annealing in the Ferromagnetic Ising Model

Alexander I. Nesterov* and Juan Carlos Beas Zepeda†
*Departamento de Física, CUCEI, Universidad de Guadalajara,
Av. Revolución 1500, Guadalajara, CP 44420, Jalisco, México*

Gennady P. Berman‡
Theoretical Division, Los Alamos National Laboratory, Los Alamos, NM 87544, USA
(Dated: April 1, 2013)

We developed a non-Hermitian quantum optimization algorithm to find the ground state of the ferromagnetic Ising model with up to 1024 spins (qubits). Our approach leads to significant reduction of the annealing time. Analytical and numerical results demonstrate that the total annealing time is proportional to $\ln N$, where N is the number of spins. This encouraging result is important in using classical computers in combination with quantum algorithms for the fast solutions of NP-complete problems. Additional research is proposed for extending our dissipative algorithm to more complicated problems.

PACS numbers: 03.67.Ac, 64.70.Tg, 03.65.Yz, 75.10.Jm

Keywords: critical points; ground states; quantum theory; adiabatic quantum computation; quantum annealing

I. INTRODUCTION

Quantum annealing (QA) algorithms can be useful for solving many hard problems related to finding the global minimum of multi-valued functions, cost functions, optimal configurations of complex networks, and the ground states of the corresponding Hamiltonians. The main idea of QA is to utilize the collective quantum tunneling effects enabling complex systems to tunnel during the slow time-evolution from local minima to the global ground state. Although many useful results have been obtained in this field, many problems still need to be resolved. The main challenge is to accelerate the speed of QA algorithms so that the annealing time grows not exponentially but polynomially with the size of the problem [1–10].

There are many approaches to finding the ground state of the Hamiltonian, \mathcal{H}_0 , using QA algorithms [1–7]. One of these approaches is based on introducing a time-dependent Hamiltonian, $\mathcal{H}(t) = \mathcal{H}_0 + \Gamma(t)\mathcal{H}_1$, where \mathcal{H}_0 is the Hamiltonian to be optimized, \mathcal{H}_1 is an auxiliary (“initial”) Hamiltonian and $[\mathcal{H}_0, \mathcal{H}_1] \neq 0$. The term $\Gamma(t)\mathcal{H}_1$ provides the non-trivial quantum dynamics required during annealing. The external time-dependent field, $\Gamma(t)$, is a control parameter that decreases from a large enough value to zero during the evolution. The ground state of \mathcal{H}_1 is the initial state. If $\Gamma(t)$ decreases sufficiently slowly, the adiabatic theorem guarantees finding the ground state of the main Hamiltonian, \mathcal{H}_0 , at the end of computation.

The main obstacles in implementation of QA algo-

gorithms in a classical computer are: (i) The efficiency of QA algorithm is limited by the exponential small energy gap between ground and excited states. For instance, in the commonly used quantum optimization m -qubit models the minimal energy gap is $g_m \approx 2^{-m/2}$ [2, 4, 11–13]. This causes the annealing time to increase exponentially with the size of the system. (ii) Direct simulations are limited to small-size problems, since it requires tracking the amplitudes of all possible classical configurations, whose number grows exponentially with system size. To overcome this problem one may use, for instance, the quantum Monte-Carlo method to simulate some stochastic dynamics to reach a ground state [4].

In [14] we proposed an alternate adiabatic quantum optimization algorithm based on the non-Hermitian quantum mechanics. Recently, we applied this non-Hermitian quantum annealing (NQA) algorithm to Grover’s problem of finding a marked item in an unsorted database [15]. We showed that a search time depends on the chosen relaxation parameters, and is proportional to the logarithm of the number of qubits.

In this paper we apply the NQA algorithm to study real-time dynamics in the one-dimensional dissipative ferromagnetic Ising spin chain. We assume that the dissipation vanishes at the end of evolution. So, after the annealing is finished, the system is governed by the Hermitian Hamiltonian. We show that a dissipation significantly increases the probability for the system to remain in the ground state. In particular, a comparison with the results of the Hermitian QA reveals that the NQA reaches the ground state of \mathcal{H}_0 with much larger probability, if we use the same annealing scheme. We show that the NQA has a complexity of order, $\ln N$, where N is the number of spins. This is much better than the quantum Hermitian adiabatic algorithm yielding the complexity of order N^2 .

A dissipative term which we use corresponds to a tun-

*Electronic address: nesterov@cencar.udg.mx

†Electronic address: juancarlosbeas@gmail.com

‡Electronic address: gpb@lanl.gov

neling of the system to its own continuum, as usually happens when one applies a Feshbach projection method on intrinsic states in nuclear physics and quantum optics. In our case, the intrinsic states are the states of the quantum computer. So, the absolute probability of our quantum computer to survive during the NQA can be small. That is why we use a ratio of two probabilities – the probability for the system to remain in the ground state to the probability of survival of the quantum computer. This relative probability (we call it “intrinsic” probability) is well-defined, and remains finite during the NQA. So, our approach cannot be directly used in the experiments on QA, but rather as a combination of classical computer and NQA to significantly decrease the time of annealing. Also, a dissipative term which we use in this paper is rather artificial in a sense that it has no a direct relation to a real physical dissipative mechanisms. At the same time, we note that our dissipation term corresponds, in principal, to the tunneling effects in the superconducting phase qubits if tunneling is realized mostly from the lowest energy levels. Our hope is that a reduction of the calculation annealing time can help to boost solution of the NP-complete problems by using combination of classical computers and NQA algorithms.

This paper is organized as follows. In Sec. II, the generic adiabatic quantum optimization (AQO) algorithm based on non-Hermitian QA is discussed. In Sec. III, we introduce a lossy one-dimensional Ising system in a transverse magnetic field governed by a non-Hermitian Hamiltonian. In Sec. IV, we study the quench dynamics of our system using both analytic and numerical methods. We conclude in Sec. V with a discussion of our results. In the Appendices we present some technical details.

II. NON-HERMITIAN QUANTUM ANNEALING: PRELIMINARIES

The generic adiabatic quantum optimization problem based on the QA algorithm can be formulated as follows [3]. Let \mathcal{H}_0 be the Hamiltonian whose ground state is to be found, and \mathcal{H}_1 be an auxiliary “initial” Hamiltonian. We consider the following time-dependent Hamiltonian:

$$\mathcal{H}_\tau(t) = \mathcal{H}_0 + g(t)\mathcal{H}_1, \quad (1)$$

where $[\mathcal{H}_0, \mathcal{H}_1] \neq 0$. The function, $g(t)$, is monotonic and satisfies the relation, $g(\tau) = 0$. It is assumed that \mathcal{H}_1 is dominant at the initial time $t = 0$, and, since $g(\tau) = 0$, the $\mathcal{H}_\tau(t) \rightarrow \mathcal{H}_0$ as $t \rightarrow \tau$.

The evolution of the system is determined by the Schrödinger equation:

$$i \frac{\partial}{\partial t} |\Psi(t)\rangle = \mathcal{H}_\tau(t) |\Psi(t)\rangle. \quad (2)$$

The initial conditions are imposed as follows: $|\Psi(0)\rangle = |\Psi_g\rangle$, where $|\Psi(0)\rangle$ is the ground state of \mathcal{H}_1 . The adiabatic theorem guarantees that the initial state, $|\Psi_g\rangle$,

evolves into the final state of $|\Psi_g(\tau)\rangle$, which is the ground state of the Hamiltonian, \mathcal{H}_0 , as long as the instantaneous ground state of $\mathcal{H}_\tau(t)$ does not become degenerate at any time.

The validity of the adiabatic theorem requires

$$\sum_{m \neq n} \left| \frac{\langle \psi_m | \partial \mathcal{H}_\tau / \partial t | \psi_n \rangle}{(E_m - E_n)^2} \right| \ll 1. \quad (3)$$

This restriction is violated near the degeneracy in which the eigenvalues coalesce. In the common case of double degeneracy with two linearly independent eigenvectors, the energy surfaces form the sheets of a double cone. The apex of the cones is called the “diabolic point”, and since, for a generic Hermitian Hamiltonian, the co-dimension of the diabolic point is three, it can be characterized by three parameters [16, 17]. For the quantum optimization governed by the Hamiltonian of Eq. (1), the requirement (3) can be written as [3, 4]

$$\tau \gg \tau_0 = \frac{\max |\langle \psi_e | \partial \mathcal{H}_\tau / \partial s | \psi_g \rangle|}{\min |E_e - E_g|^2}, \quad (4)$$

where $s = t/\tau$, and E_e is the energy of the first excited state, $|\psi_e\rangle$. Thus, if at the time, $\tau_c < \tau$, the gap, $\Delta E = |E_e - E_g|$, is small enough, the time required to pass from the initial state to the final state becomes very large, and the AQO loses its advantage over thermal annealing.

Recently [14], we proposed a generic non-Hermitian adiabatic quantum optimization. Here we consider a particular case of the NQA. Let \mathcal{H}_0 be a Hamiltonian whose ground state is to be found, and let,

$$\tilde{\mathcal{H}}_1(t) = g(1 - t/\tau)\mathcal{H}_1 - i\delta(1 - t/\tau)\mathcal{H}_2, \quad (5)$$

be the non-Hermitian auxiliary “initial” Hamiltonian.

Consider the following time-dependent Hamiltonian:

$$\tilde{\mathcal{H}}_\tau(t) = \mathcal{H}_0 + \tilde{\mathcal{H}}_1(t), \quad (6)$$

where $[\mathcal{H}_0, \mathcal{H}_1(0)] \neq 0$. We impose the initial conditions as follows: $|\Psi(0)\rangle = |\Psi_g\rangle$, so that $\tilde{\mathcal{H}}_1|\psi_g\rangle = E_g|\psi_g\rangle$ with E_g being the energy of the ground state of the auxiliary non-Hermitian Hamiltonian $\tilde{\mathcal{H}}_1$. At the end of evolution the total Hamiltonian $\tilde{\mathcal{H}}_\tau(\tau) = \mathcal{H}_0$, and the adiabatic theorem provides that the final state be the ground state of \mathcal{H}_0 , if the evolution was slow enough.

We denote by $|\psi_n(t)\rangle$ and $\langle \tilde{\psi}_n(t)|$ the right and left instantaneous eigenvectors of the total Hamiltonian: $\tilde{\mathcal{H}}_\tau(t)|\psi_n(t)\rangle = E_n(t)|\psi_n(t)\rangle$, $\langle \tilde{\psi}_n(t)|\tilde{\mathcal{H}}_\tau(t) = \langle \tilde{\psi}_n(t)|E_n(t)$. We assume that these eigenvectors form a bi-orthonormal basis, $\langle \tilde{\psi}_m|\psi_n\rangle = \delta_{mn}$ [18].

For the non-Hermitian quantum optimization problem governed by the Hamiltonian (6), the validity of adiabatic approximation requires

$$\tau \gg \frac{\max |\langle \tilde{\psi}_e | \dot{\tilde{\mathcal{H}}}_\tau(t) | \psi_g \rangle|}{\min |E_e(t) - E_g(t)|^2}, \quad (7)$$

where the “dot” denotes the derivative with respect to the dimensionless time, $s = t/\tau$. This restriction is violated near the ground state degeneracy, where complex energy levels cross. The point of degeneracy is known as the exceptional point, and it is characterized by a coalescence of eigenvalues and their corresponding eigenvectors, as well. Therefore, studying the behavior of the system in the vicinity of the exceptional point requires a special care [19–21].

In the vicinity of the level crossing point, only the two-dimensional Jordan block, related to the level crossing, makes the most considerable contribution to the quantum evolution. Then, the multi-dimensional problem can be described by the effective two-dimensional Hamiltonian, acting in the subspace spanned by the ground state and the first excited state of the total non-Hermitian Hamiltonian, \tilde{H}_τ [14].

III. DESCRIPTION OF THE MODEL

In this section, we consider the one-dimensional Ising model in a transverse magnetic field with dissipation governed by the following non-Hermitian Hamiltonian:

$$H = -\frac{J}{2} \sum_{n=1}^N (g\sigma_n^x + \sigma_n^z \sigma_{n+1}^z + i2\delta\sigma_n^- \sigma_n^+), \quad (8)$$

with periodic boundary condition, $\sigma_{N+1} = \sigma_1$. The external magnetic field is associated with the parameter, g , the rate of decay is described by the parameter, δ , and $\sigma_n^\pm = (\sigma_n^z \pm i\sigma_n^y)/2$ are the spin raising and lowering operators.

In principle, this model can be realized in a chain of the superconducting phase qubits with the tunneling to the continuum mostly from the lowest energy levels, and by applying the standard Feshbach projection method to obtain effective non-Hermitian Hamiltonian. To get the Hamiltonian of Eq. (8) one needs to make rotation along the axes y by $\pi/2$ radians.

We apply the standard Jordan-Wigner transformation, and the following procedure outlined in [22–25],

$$\sigma_n^x = 1 - 2c_n^\dagger c_n, \quad (9)$$

$$\sigma_n^y = i(c_n^\dagger - c_n) \prod_{m<n} (1 - 2c_m^\dagger c_m), \quad (10)$$

$$\sigma_n^z = -(c_n + c_n^\dagger) \prod_{m<n} (1 - 2c_m^\dagger c_m), \quad (11)$$

in which c_n are fermionic operators that satisfy anti-commutation relations: $\{c_m^\dagger, c_n\} = \delta_{mn}$ and $\{c_m, c_n\} = \{c_m^\dagger, c_n^\dagger\} = 0$. Then, we obtain $H = P^+ H^+ P^+ + P^- H^- P^-$, where

$$P^\pm = \frac{1}{2} \left(1 \pm \prod_{n=1}^N (1 - 2c_n^\dagger c_n) \right) \quad (12)$$

denote the projectors onto the subspaces with even “+” and odd “−” numbers of quasiparticles [22, 26], and

$$H^\pm = -\frac{J}{2} \sum_{n=1}^N (c_n^\dagger c_{n+1} + c_{n+1} c_n + \tilde{g} + i\delta - 2\tilde{g}c_n^\dagger c_n + c_{n+1}^\dagger c_n + c_n^\dagger c_{n+1}^\dagger), \quad (13)$$

in which $\tilde{g} = g + i\delta$.

The Hamiltonian, H^- , is related to c_n ’s with the periodic boundary conditions, $c_{N+1} = c_1$, while in H^+ the operators, c_n , obey the following (‘antiperiodic’) boundary conditions: $c_{N+1} = -c_1$. Since the parity of quasiparticles is conserved, one can consider only either H^+ or H^- . Further we consider only quasiparticles with the even parity.

Applying the Fourier transformations with the antiperiodic boundary condition, $c_{N+1} = -c_1$,

$$c_n = \frac{e^{-i\pi/4}}{\sqrt{N}} \sum_k c_k e^{in\varphi_k}, \quad (14)$$

$$\varphi_k = \frac{2\pi k}{N}, \quad k = \pm\frac{1}{2}, \pm\frac{3}{2}, \dots, \pm\frac{N-1}{2}, \quad (15)$$

we obtain, $H^+ = \sum_k H_k$, where

$$H_k = \frac{J}{2} (2(\tilde{g} - \cos \varphi_k) c_k^\dagger c_k - \tilde{g} - i\delta + \sin \varphi_k (c_k^\dagger c_{-k}^\dagger + c_{-k} c_k)). \quad (16)$$

The Hamiltonian, H^+ , can be diagonalized by using the generalized Bogoliubov transformation:

$$c_k = \cos \frac{\theta_k}{2} b_k + \sin \frac{\theta_k}{2} b_{-k}^\dagger, \quad (17)$$

$$c_k^\dagger = \cos \frac{\theta_k}{2} b_k^\dagger + \sin \frac{\theta_k}{2} b_{-k}, \quad (18)$$

$$b_k = \cos \frac{\theta_k}{2} c_k + \sin \frac{\theta_k}{2} c_{-k}^\dagger, \quad (19)$$

$$b_k^\dagger = \cos \frac{\theta_k}{2} c_k^\dagger + \sin \frac{\theta_k}{2} c_{-k}, \quad (20)$$

where

$$\cos \theta_k = \frac{\tilde{g} - \cos \varphi_k}{\sqrt{\tilde{g}^2 - 2\tilde{g} \cos \varphi_k + 1}}, \quad (21)$$

$$\sin \theta_k = \frac{\cos \varphi_k}{\sqrt{\tilde{g}^2 - 2\tilde{g} \cos \varphi_k + 1}}, \quad (22)$$

with θ_k being a complex angle.

There are two eigenstates for each k ,

$$|u_+(k)\rangle = \begin{pmatrix} \cos \frac{\theta_k}{2} \\ \sin \frac{\theta_k}{2} \end{pmatrix}, \quad \langle \tilde{u}_+(k) | = \left(\cos \frac{\theta_k}{2}, \sin \frac{\theta_k}{2} \right), \quad (23)$$

$$|u_-(k)\rangle = \begin{pmatrix} -\sin \frac{\theta_k}{2} \\ \cos \frac{\theta_k}{2} \end{pmatrix}, \quad \langle \tilde{u}_-(k) | = \left(-\sin \frac{\theta_k}{2}, \cos \frac{\theta_k}{2} \right), \quad (24)$$

with the complex energies, $\varepsilon_{\pm}(k) = -\varepsilon_0(k) \pm \varepsilon_k$, where $\varepsilon_0(k) = J \cos \varphi_k + iJ\delta$, and $\varepsilon_k = J\sqrt{\tilde{g}^2 - 2\tilde{g} \cos \varphi_k + 1}$. Here we denote by $|u_{\pm}(k)\rangle$ ($|\tilde{u}_{\pm}(k)\rangle$) the right (left) eigenvectors.

With help of Eqs. (17) – (20) we obtain the diagonalized Hamiltonian as a sum of quasiparticles with half-integer quasimomenta,

$$\begin{aligned} H^+ &= -\frac{1}{2} \sum_k \varepsilon_0(k) + \sum_k \varepsilon_k \left(b_k^\dagger b_k - \frac{1}{2} \right) \\ &= -\sum_{k>0} \varepsilon_0(k) + \sum_{k>0} \varepsilon_k \left(b_k^\dagger b_k - b_{-k} b_{-k}^\dagger \right). \end{aligned} \quad (25)$$

Its spectrum contains only states with even number of quasiparticles.

The ground state of the Hamiltonian (25) is a state, $|\psi_g\rangle$, annihilated by all quasiparticles annihilation operators, b_k , so that, $b_k|\psi_g\rangle = 0$. One can show that the ground state can be written as a product of qubit-like states:

$$|\psi_g\rangle = \bigotimes_k \left(\cos \frac{\vartheta_k}{2} |0\rangle_k |0\rangle_{-k} - \sin \frac{\vartheta_k}{2} |1\rangle_k |1\rangle_{-k} \right), \quad (26)$$

$$\langle \tilde{\psi}_g | = \bigotimes_k \left(\cos \frac{\vartheta_k}{2} \langle 0|_k \langle 0|_{-k} - \sin \frac{\vartheta_k}{2} \langle 1|_k \langle 1|_{-k} \right), \quad (27)$$

where $|0\rangle_k$ is the vacuum state of the mode c_k , and $|1\rangle_k$ is the excited state: $|1\rangle_k = c_k^\dagger |0\rangle_k$.

Since for each k , the ground state lies into the two-dimensional Hilbert space spanned by $|0\rangle_k |0\rangle_{-k}$ and $|1\rangle_k |1\rangle_{-k}$, it is sufficient to project H_k on this subspace. For a given value of k , both of these states can be represented as a point on the complex two-dimensional sphere, S_c^2 . In this subspace the Hamiltonian, H_k , takes the form

$$H_k = -\varepsilon_0(k) \mathbb{1} + J \begin{pmatrix} \tilde{g} - \cos \varphi_k & \sin \varphi_k \\ \sin \varphi_k & -\tilde{g} + \cos \varphi_k \end{pmatrix}. \quad (28)$$

For $|\tilde{g}| \gg 1$, the ground state is paramagnetic with all spins oriented along the x axis, and from Eq. (21) we obtain $\cos \theta_k \rightarrow 1$ as $|\tilde{g}| \rightarrow \infty$. Thus, the south pole of the complex Bloch sphere corresponds to the paramagnetic ground state. On the other hand, when $|g| \ll 1$ there are two degenerate ferromagnetic ground states with all spins polarized either up or down along the z axis. The real part of the complex energy reaches its minimum at the point defined by $\cos \theta_k = -1$, and, hence, the north pole of the complex sphere is related to the pure ferromagnetic ground state with the broken symmetry in which all spins have orientation either up or down. However, in the thermodynamic limit the system passing through the critical point ends in a superposition of up and down states with finite domains of spins separated by kinks [23].

In the thermodynamic limit the absolute value of the difference between the two eigenvalues of the Hamiltonian (28) is given by

$$|\Delta\varepsilon| = 2J|\sqrt{\tilde{g}^2 - 2\tilde{g} \cos \vartheta + 1}|, \quad (29)$$

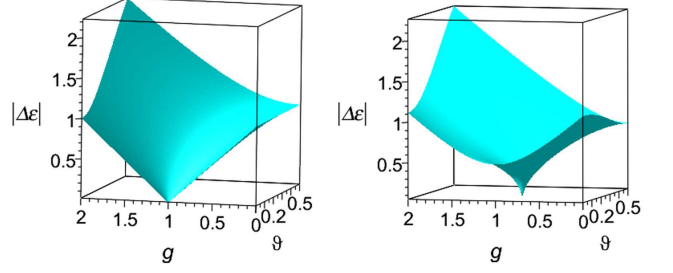


FIG. 1: (Color online) Absolute value of difference, $|\Delta\varepsilon|$, of the eigenvalues of the Hamiltonian (28) as function of g and ϑ . Left panel: $\delta = 0$. Right panel: $\delta = 0.25$.

where $\varphi_k \rightarrow \vartheta$ as $N \rightarrow \infty$. As one can see in Fig. 1, the energy gap vanishes at the critical point,

$$\vartheta_c = \arccos \sqrt{1 - \delta^2}, \quad (30)$$

$$g_c = \sqrt{1 - \delta^2}. \quad (31)$$

The difference between the Hermitian QA and non-Hermitian QA is that, while in the first case the gap vanishes for long wavelength modes ($\vartheta_c = 0$), in the second case the minimal gap shifts to short wavelength modes ($\vartheta_c = \arccos \sqrt{1 - \delta^2}$).

In the thermodynamic limit the ground state energy per spin can be written as

$$\varepsilon_{gs} = -\frac{1}{2\pi} \int_0^\pi \left(\varepsilon_0(\vartheta) + J\sqrt{\tilde{g}^2 - 2\tilde{g} \cos \vartheta + 1} \right) d\vartheta. \quad (32)$$

Performing the integration, we obtain

$$\varepsilon_{gs} = -\frac{iJ\delta}{2} - \frac{J(\tilde{g} + 1)}{2\pi} \mathbf{E}(2\sqrt{\tilde{g}}/(\tilde{g} + 1)), \quad (33)$$

where $\mathbf{E}(z)$ denotes a complete elliptic integral of the second kind.

IV. QUENCH DYNAMICS

In this section, we consider the NQA for the time-dependent Hamiltonian of Eq.(8) written as

$$\tilde{\mathcal{H}}_\tau(t) = \mathcal{H}_0 + \mathcal{H}_1(t), \quad (34)$$

where

$$\mathcal{H}_0 = -\frac{J}{2} \sum_{n=1}^N \sigma_n^z \sigma_{n+1}^z, \quad (35)$$

$$\mathcal{H}_1(t) = -\frac{J}{2} \sum_{n=1}^N (g(t) \sigma_n^x + i2\delta(t) \sigma_n^- \sigma_n^+). \quad (36)$$

We start with the ground state of the auxiliary Hamiltonian, $\mathcal{H}_1(0)$, as the initial state, which is a “paramagnetic” with all spins oriented along the x axis. For $g \gg 1$

the Hamiltonian, $\mathcal{H}_\tau(0)$, is dominated by $\mathcal{H}_1(0)$, and the ground state of the total Hamiltonian, $\tilde{\mathcal{H}}_\tau$, is determined by the ground state of $\mathcal{H}_1(0)$. The \mathcal{H}_1 term causes quantum tunneling between the eigenstates of the Hamiltonian, \mathcal{H}_0 . At the end of NQA we obtain, $\tilde{\mathcal{H}}_\tau(\tau) = \mathcal{H}_0$. If the quench is slowly enough, the adiabatic theorem guarantees reaching the ground state of the main Hamiltonian, \mathcal{H}_0 , at the end of computation.

As shown in the Sec. III, the total Hamiltonian, $\tilde{\mathcal{H}}_\tau(t)$, in the momentum representation splits into a sum of independent terms, $\tilde{\mathcal{H}}_\tau(t) = \sum_k \mathcal{H}_k(t)$. Each \mathcal{H}_k acts in the two-dimensional Hilbert space spanned by $|k_1\rangle = |1\rangle_k |1\rangle_{-k}$ and $|k_0\rangle = |0\rangle_k |0\rangle_{-k}$. The wave function can be written as, $|\psi\rangle = \prod_k |\psi_k\rangle$, where

$$|\psi_k(t)\rangle = c_0(k, t)|k_0\rangle + c_1(k, t)|k_1\rangle. \quad (37)$$

Choosing the basis as, $|k_1\rangle = \begin{pmatrix} 1 \\ 0 \end{pmatrix}$ and $|k_0\rangle = \begin{pmatrix} 0 \\ 1 \end{pmatrix}$, we find that the Hamiltonian, $\mathcal{H}_k(t)$, projected on this two-dimensional subspace takes the form

$$\mathcal{H}_k(t) = -\varepsilon_0(t)\mathbb{1} + J \begin{pmatrix} \tilde{g}(t) - \cos \varphi_k & \sin \varphi_k \\ \sin \varphi_k & -\tilde{g}(t) + \cos \varphi_k \end{pmatrix}, \quad (38)$$

where $\varepsilon_0(t) = J \cos \varphi_k + iJ\delta(t)$ and $\tilde{g}(t) = g(t) + i\delta(t)$. Further we assume linear dependence of $\tilde{g}(t)$ on time:

$$\tilde{g}(t) = \begin{cases} \gamma(\tau - t), & 0 \leq t \leq \tau \\ 0, & t > \tau \end{cases} \quad (39)$$

where $\gamma = (g + i\delta)/\tau$, and g, δ are real parameters.

A. Diabatic basis

The general wave functions, $|\psi_k\rangle$ and $\langle\tilde{\psi}_k|$, satisfy the Schrödinger equation and its adjoint equation

$$i\frac{\partial}{\partial t}|\psi_k\rangle = \mathcal{H}_k(t)|\psi_k\rangle, \quad (40)$$

$$-i\frac{\partial}{\partial t}\langle\tilde{\psi}_k| = \langle\tilde{\psi}_k|\mathcal{H}_k(t). \quad (41)$$

Presenting $|\psi_k(t)\rangle$ as a linear superposition,

$$|\psi_k(t)\rangle = (u_k(t)|k_0\rangle + v_k(t)|k_1\rangle)e^{i\int \varepsilon_0(t)dt}, \quad (42)$$

and inserting expression (42) into Eq. (40), we obtain

$$i\dot{u}_k = J(-(\tilde{g} - \cos \varphi_k)u_k + \sin \varphi_k v_k), \quad (43)$$

$$i\dot{v}_k = J(\sin \varphi_k u_k + (\tilde{g} - \cos \varphi_k)v_k). \quad (44)$$

The solution can be written in terms of the parabolic cylinder functions, $D_{-i\nu_k}(\pm z)$. (For details see Appendix A.):

$$U_k(z_k) = B_k D_{-i\nu_k}(z_k) - i\sqrt{i\nu_k} A_k D_{i\nu_k-1}(iz_k), \quad (45)$$

$$V_k(z_k) = A_k D_{i\nu_k}(iz_k) - \sqrt{i\nu_k} B_k D_{-i\nu_k-1}(z_k), \quad (46)$$

in which we introduced new functions: $u_k(t) = U(z_k)$, $v_k(t) = V(z_k)$ and

$$z_k(t) = e^{i\pi/4} \sqrt{\frac{2J}{\gamma}} (\gamma(\tau - t) - \cos \varphi_k), \quad (47)$$

$$\nu_k = \frac{J \sin^2 \varphi_k}{2\gamma}. \quad (48)$$

The constants, A_k and B_k in Eqs. (45), (46), are determined by the initial conditions.

In what follows we assume that the evolution of the spin chain starts at $t_0 = 0$ in the ‘ground’ state. This implies that for each k the evolution of the corresponding two-level system (TLS) starts from the state, $|\psi(0)\rangle = |k_0\rangle$. Then, the following initial conditions should be imposed: $u_k(0) = 1$ and $v_k(0) = 0$. The related boundary condition are, $z_k(0) = e^{i\pi/4} \sqrt{2J/\gamma} (\gamma\tau - \cos \varphi_k)$. Using these conditions, we obtain the solution of the Schrödinger equation as follows. (See Appendix A for details.):

$$U_k(z_k) = B_k D_{-i\nu_k}(z_k), \quad (49)$$

$$V_k(z_k) = -\sqrt{i\nu_k} B_k D_{-i\nu_k-1}(z_k), \quad (50)$$

where $B_k = e^{\pi\nu_k/2} D_{i\nu_k}(iz_k(0))$.

It is assumed that a quantum measurement will determine the state of the quantum system at $t > \tau$, when the external field, $\tilde{g}(t) = 0$. We denote the final state of the system, at $t = \tau$, as $|\psi_\tau\rangle = \prod_k |\psi_k(\tau)\rangle$. The probability, $P_n(k)$, of finding the TLS in a given state, $|k_n\rangle$ ($n = 0, 1$), can be written as

$$P_n(k) = \frac{| \langle k_n | \psi_\tau \rangle |^2}{| \langle \psi_\tau | \psi_\tau \rangle |^2}. \quad (51)$$

Since for non-Hermitian systems the norm of the wavefunction is not conserved, we define the (intrinsic) probability of transition, $|k_0\rangle \rightarrow |k_1\rangle$, as

$$P_k(t) = \frac{|v_k(t)|^2}{|u_k(t)|^2 + |v_k(t)|^2}. \quad (52)$$

Using the functions, $U(z_k)$ and $V(z_k)$, we recast (52) as

$$P_k(t) = \frac{1}{1 + \frac{|D_{-i\nu_k}(z_k(t))|^2}{|\sqrt{i\nu_k} D_{-i\nu_k-1}(z_k(t))|^2}}. \quad (53)$$

To calculate $P_k(t)$ at the end of evolution ($t = \tau$) we use asymptotic formulas of the Weber functions. For large values of the argument, $|z_k(\tau)| = |\sqrt{2J/\gamma} \cos \varphi_k| \gg 1$, one can apply the asymptotic formulas for parabolic cylinder functions to estimate the probability of transition. For $\tau \gg 1$ the modulus of this argument is large for most k , except near $\varphi_k = \pm\pi/2$.

For wavelength modes with $\varphi_k \ll \pi/4$, using the asymptotic formulas for the Weber functions, we obtain

$$\frac{D_{-i\nu_k}(z_k(\tau))}{\sqrt{i\nu_k} D_{-i\nu_k-1}(z_k(\tau))} \approx \frac{e^{-\pi\nu_k/2} e^{-z_k^2(\tau)/2} \Gamma(1 + i\nu_k)}{\sqrt{2\pi i\nu_k}}. \quad (54)$$

Inserting (54) into Eq. (53), we obtain

$$P_k(\tau) = \frac{1}{1 + \frac{|\Gamma(1 + i\nu_k)|^2}{2\pi|\nu_k|} e^{-\pi\Re\nu_k - \Re z_k^2(\tau)}}. \quad (55)$$

For $\delta \ll g$ we can approximate $\Gamma(1 + i\nu) \approx \Gamma(1 + i\Re\nu)$. Next, using the relation [27],

$$|\Gamma(iy)|^2 = \frac{\pi}{y \sinh \pi y}, \quad (56)$$

for real y , we obtain

$$P_k(\tau) = \frac{1 - e^{-2\pi\Re\nu_k}}{1 - e^{-2\pi\Re\nu_k} + e^{-2\pi\Re\nu_k - \Re z_k^2(\tau)}}. \quad (57)$$

In the case of the Hermitian QA ($\delta = 0$), one has $\Re z_k^2(\tau) = 0$, and Eq. (55) leads to the Landau-Zener formula [28, 29],

$$P_k(\tau) = 1 - e^{-(\pi J\tau/g) \sin^2 \varphi_k}. \quad (58)$$

To calculate the transition probability for $\varphi_k \approx \pi/2$ we use the expansion for small value of the argument of Weber function, $|z_k| \ll 1$ (see Eq. (A44)). The computation yields

$$P_{\pi/2}(\tau) = \frac{1}{1 + \frac{|\Gamma(\frac{i\nu_k}{2})|^2}{|\Gamma(\frac{1+i\nu_k}{2})|^2}}. \quad (59)$$

For the Hermitian QA this gives

$$P_{\pi/2}(\tau) = \frac{\tanh \pi\nu/2}{1 + \tanh \pi\nu/2}, \quad (60)$$

in which $\nu = J\tau/(2g)$. From Eq. (60) it follows that for $\tau \gg g/J$ the probability $P_{\pi/2}(\tau) \simeq 1/2$.

In Fig. 2 we present the results of our numerical simulation for $N = 1024$ qubits. As one can see, for long wavelength modes with $\varphi_k \ll \pi/4$ (blue and red lines), the NQA shows better performance than the Hermitian QA. For $\varphi_k = \pi/2$ the probability of transition is $P_{\pi/2}(\tau) \simeq 1/2$ for both schedules, either Hermitian QA or non-Hermitian QA (orange line).

B. Adiabatic basis

A widely used opinion is that for slowly enough evolution the only long wavelength modes become excited (see e.g. [23]). However, as it was shown in the Subsection A, even for the Hermitian QA, the transition probability, $P_k \approx 1/2$, for $k \approx \pi/2$. Thus, it is not clear what is the contribution of the short wavelength modes ($k \sim \pi/2$) to the probability of the whole system to stay in the ground state. To respond to this question we consider the expansion of the wavefunction, $|\psi\rangle = \prod_k |\psi_k(t)\rangle$, in the

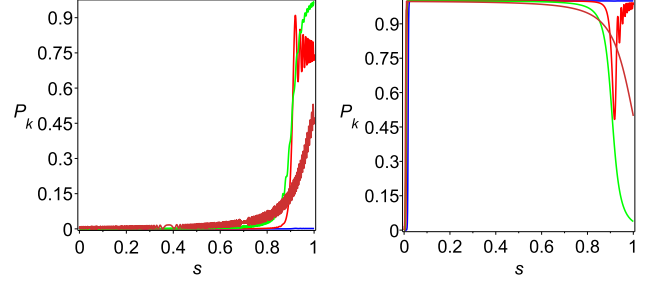


FIG. 2: The probability of transition (remain in the ground state), $|k_0\rangle \rightarrow |k_1\rangle$, as a function of the scaled time, $s = t/\tau$ ($J = 0.5$, $g = 10$, $\tau = 10^3$, $N = 1024$, $k = p - 1/2$). Left panel: Hermitian QA ($\delta = 0$). From bottom to top: $p = 1, 256, 16, 64$. Right panel: NQA ($\delta = 0.5$). From top to bottom: $p = 1, 16, 256, 64$.

adiabatic basis, formed by the instantaneous eigenvectors.

In the adiabatic basis the wavefunction, $|\psi_k(t)\rangle$, can be written as follows:

$$|\psi_k(t)\rangle = \alpha_k(t)|u_-(k, t)\rangle + \beta_k(t)|u_+(k, t)\rangle. \quad (61)$$

We assume that the evolution begins from the ground state that implies, $\alpha_k(0) = 1$ and $\beta_k(0) = 0$. At the end of evolution at $t = \tau$, when $\tilde{g} = 0$, we have

$$|\psi_k(\tau)\rangle = \alpha_k(\tau)|u_-(k, \tau)\rangle + \beta_k(\tau)|u_+(k, \tau)\rangle, \quad (62)$$

where

$$|u_+(k, \tau)\rangle = \begin{pmatrix} \sin \frac{\varphi_k}{2} \\ \cos \frac{\varphi_k}{2} \end{pmatrix}, \quad (63)$$

$$|u_-(k, \tau)\rangle = \begin{pmatrix} -\cos \frac{\varphi_k}{2} \\ \sin \frac{\varphi_k}{2} \end{pmatrix}. \quad (64)$$

By presenting,

$$\alpha_k(t) = a_k(t) e^{-i \int_0^t \varepsilon_-(k, t) dt}, \quad (65)$$

$$\beta_k(t) = b_k(t) e^{-i \int_0^t \varepsilon_+(k, t) dt}, \quad (66)$$

one can show that the coefficients, $a_k(t)$ and $b_k(t)$, satisfy the following asymptotic conditions:

$$a_k(\tau) = 1 + \mathcal{O}(1/\tau), \quad (67)$$

$$b_k(\tau) = \mathcal{O}\left(\exp\left(2\tau \Im \int_0^{z_c} \varepsilon_k(z) dz\right)\right), \quad (68)$$

where the critical point, z_c , lies on the first Stokes line in the *lower* complex line defined as

$$\Im \int_0^{z_c} \varepsilon_k(z) dz < 0. \quad (69)$$

Here the critical point, z_c , is determined as a solution of the equation, $\varepsilon_k(z_c) = 0$, in the complex plane obtained by analytical continuation, $t \rightarrow z$ [30–38].

Similarly, if initially the system was in the excited state: $|\psi_k(0)\rangle = |u_+(k, 0)\rangle$, so that $\alpha_k(0) = 0$ and $\beta_k(0) = 1$, the result of integration yields

$$b_k(\tau) = 1 + \mathcal{O}(1/\tau), \quad (70)$$

$$a_k(\tau) = \mathcal{O}\left(\exp\left(2\tau\Im\int_0^{z_c}\varepsilon_k(z)dz\right)\right). \quad (71)$$

The intrinsic probability to remain in the ground state at the end of the adiabatic evolution is given by

$$P_k^{gs}(\tau) = \frac{|\alpha_k(\tau)|^2}{|\alpha_k(\tau)|^2 + |\beta_k(\tau)|^2}. \quad (72)$$

With help of Eqs. (65), (66) we obtain

$$P_k^{gs}(\tau) = \frac{1}{1 + \frac{|b_k(\tau)|^2}{|a_k(\tau)|^2} e^{4\Im\int_0^\tau\varepsilon_k(t)dt}}. \quad (73)$$

From here it follows that for any, $0 \leq t \leq \tau$, the adiabatic evolution should be performed along the path corresponding to, $\Im\varepsilon_k(t) \leq 0$. In the exact solution, given by

$$\alpha_k(\tau) = -B_k e^{-\delta\tau/2} \left(D_{-i\nu_k}(z_k(\tau)) \sin \frac{\varphi_k}{2} + \sqrt{i\nu_k} D_{-i\nu_k-1}(z_k(\tau)) \cos \frac{\varphi_k}{2} \right), \quad (74)$$

$$\beta_k(\tau) = B_k e^{-\delta\tau/2} \left(D_{-i\nu_k}(z_k(\tau)) \cos \frac{\varphi_k}{2} - \sqrt{i\nu_k} D_{-i\nu_k-1}(z_k(\tau)) \sin \frac{\varphi_k}{2} \right), \quad (75)$$

it manifests itself in the choice of phase in the argument of the Weber function, when we apply the asymptotic expansion.

The probability for the whole system to stay in the ground state at the end of the evolution is given by, $P_{gs} = \prod_k P_k^{gs}(\tau)$. For long wavelength modes with $\varphi_k \ll \pi/4$, using the asymptotic formulas for the Weber functions with the large value of its argument, we find that $P_k^{gs}(\tau) = P_k(\tau)$, where $P_k(\tau)$ is the transition probability of spin flip given by Eq. (55). For the Hermitian QA this yields the LZ result

$$P_k(\tau) = 1 - e^{-(\pi J\tau/g)\sin^2\varphi_k} \approx 1 - e^{-\pi^3 J\tau k^2/(gN^2)}. \quad (76)$$

And in the case of the NQA (for $\delta \ll g$) we obtain

$$P_k(\tau) = \frac{1 - e^{-2\pi\Re\nu_k}}{1 - e^{-2\pi\Re\nu_k} + e^{-2\pi\Re\nu_k - \Re z_k^2(\tau)}}, \quad (77)$$

where

$$\Re\nu_k \approx (J\tau/2g)\sin^2\varphi_k, \quad (78)$$

$$\Re z_k^2(\tau) \approx (2\delta J\tau/g^2)\cos^2\varphi_k. \quad (79)$$

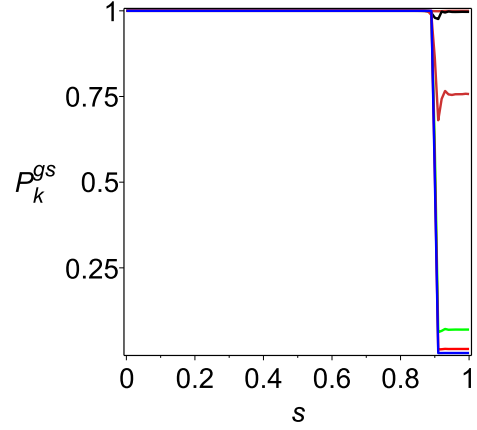


FIG. 3: (Color online) The probability, P_k^{gs} , of TLS to remain in the ground state as a function of the scaled time, $s = t/\tau$, for the Hermitian QA ($\delta = 0$, $J = 0.5$, $g = 10$, $\tau = 10^3$, $N = 1024$, $k = p - 1/2$). From bottom to top: $p = 1, 2, 4, 16, 32, 64$.

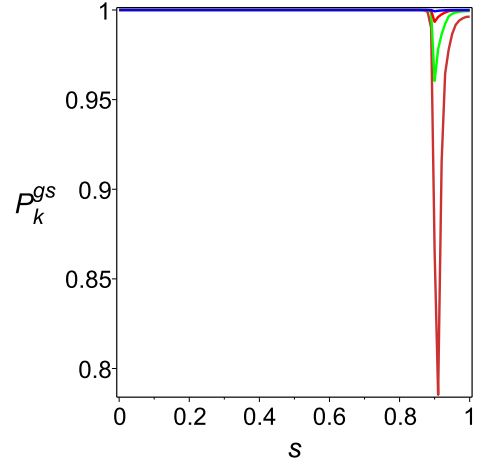


FIG. 4: (Color online) The probability, P_k^{gs} , of TLS to remain in the ground state as a function of the scaled time, $s = t/\tau$, for the NQA ($\delta = 0.5$, $J = 0.5$, $g = 10$, $\tau = 10^3$, $N = 1024$, $k = p - 1/2$). From bottom to top: $p = 1, 2, 4, 16$.

For short wavelength modes, approximately with $\pi/4 < \varphi_k \leq \pi/2$, employing the large-order asymptotics for Weber functions, we obtain $P_k^{gs}(\tau) = 1 + \mathcal{O}(1/\sqrt{|\nu_k|})$. (See Appendix A.)

Our theoretical predictions are confirmed by numerical calculations performed for $N = 1024$ qubits. (See Figs. 3, 4.) One can observe that while short wavelength excitations are essential at the critical point, at the end of evolution their contribution to the transition probability from the ground state to the first excited state is negligible.

V. PERFORMANCE CHARACTERIZATION OF THE QUANTUM ANNEALING

During the QA the system does not stay always at the ground state at all times. At the critical point, the system becomes excited, and its final state is determined by the number of defects (kinks). To evaluate the efficiency of QA one can calculate the number of defects. Then, computational time is the time required to achieve the number of defects below some acceptable value.

Following [23], we define the operator of the number of kinks as

$$\hat{\mathcal{N}} = \frac{1}{2} \sum_{n=1}^N (1 - \sigma_n^z \sigma_{n+1}^z) = \sum_k b_k^\dagger b_k. \quad (80)$$

The number of kinks, being equal to the number of quasi-particles excited at $\tilde{g} = 0$ (final state), is given by

$$\mathcal{N} = \langle \psi_\tau | \hat{\mathcal{N}} | \psi_\tau \rangle. \quad (81)$$

Eq. (81) can be recast as follows: $\mathcal{N} = E_{res}/J$, where E_{res} is the residual energy defined as the difference between the solution obtained by QA and the exact one [3, 5, 39],

$$E_{res} = \langle \psi_\tau | \mathcal{H}_0 | \psi_\tau \rangle - E_{gs}. \quad (82)$$

This leads to an alternative (equivalent) way to evaluate the efficiency of QA by calculating E_{res} . Note, that for more complicated systems that include disorder, the residual energy may not have a simple link with the density of defects [40].

Using Eq. (62), we can calculate the number of kinks as follows:

$$\mathcal{N} = \sum_k (1 - P_k^{gs}(\tau)), \quad (83)$$

where $P_k^{gs}(\tau)$ is given by Eq. (72). In the thermodynamic limit the sum in Eq. (83) can be replaced by integral, and we obtain for the density of kinks the following expression:

$$n = \lim_{N \rightarrow \infty} \frac{\mathcal{N}}{N} = \frac{1}{\pi} \int_0^\pi d\vartheta (1 - P^{gs}(\vartheta, \tau)). \quad (84)$$

As was shown in the previous section, during slow evolution only long wavelength modes can be excited. So one can use the Gaussian distribution by replacing $\sin \varphi_k \approx \varphi_k$ and $\cos \varphi_k \approx 1$. In the limit $\sqrt{2J\tau/g} \gg 1$, we can employ Eqs. (77) - (79) to calculate the number of kinks as

$$n = \frac{1}{\pi} \int_0^\pi \frac{e^{-2\pi\Re\nu - \Re z^2} d\vartheta}{1 - e^{-2\pi\Re\nu} + e^{-2\pi\Re\nu \Re z^2}}. \quad (85)$$

Performing the integration with $\Re\nu = J\tau\vartheta^2/(2g)$ and $\Re z^2 = 2\delta J\tau/g^2$, we obtain [51]

$$n = n_0 e^{-2\delta\tau J/g^2} \Phi\left(1 - e^{-2\delta\tau J/g^2}, \frac{1}{2}, 1\right), \quad (86)$$

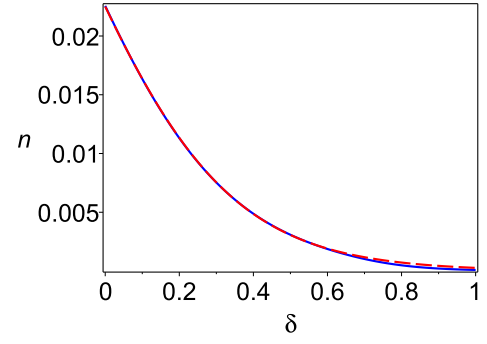


FIG. 5: (Color online) Density of kinks as function of the dissipation parameter, δ ($\tau = 10^3$, $J = 0.5$, $g = 10$, $N = 1024$). Blue line: exact result. Red dashed line: asymptotic formula of Eq. (86).

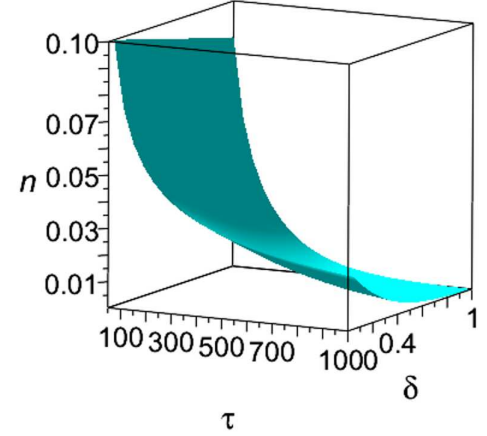


FIG. 6: (Color online) Density of kinks as function of the dissipation parameter δ and annealing time τ .

where

$$n_0 = \frac{1}{2\pi} \sqrt{\frac{g}{J\tau}} \quad (87)$$

denotes the density of kinks for the Hermitian LZ problem [23], and $\Phi(x, a, c)$ is the Lerch transcendent [41].

In Figs. 5, 6 we present the results of numerical simulation for the density of defects. In Fig. 5 the density of kinks as a function of δ is depicted. In Fig. 6 we show the dependence of the density of defects as a function of the decay parameter, δ , and annealing time, τ , in the thermodynamic limit. This is consistent with the results of numerical simulation presented in Ref. [42] for the Hermitian LZ problem.

The final state of the system is a ferromagnetic state with the finite domains of spins (pointed up or down), separated by kinks. The magnetization, Nm_z , is defined from the expression for the total energy of the ground state: $E_{gs} = -NJm_z^2$. In the thermodynamic limit, we

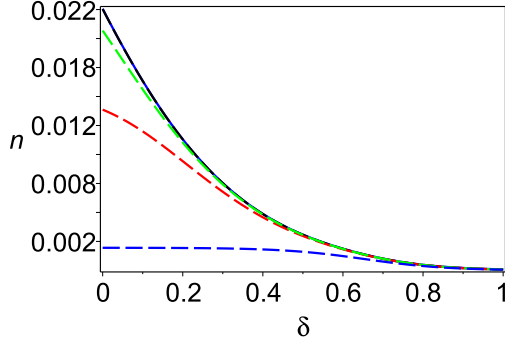


FIG. 7: (Color online) Density of kinks as function of the dissipation parameter, δ ($J = 0.5$, $g = 10$, $\tau = 10^3$, $N = 1024$). Blue solid shows the exact result. Dashed color lines present contribution of the first k -modes ($k = p - 1/2$). From bottom to top: $p = 1, 8, 16, 32$.

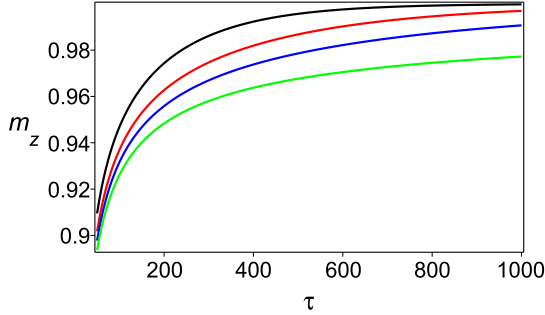


FIG. 8: (Color online) Density of magnetization, m_z , as function of the annealing time, τ . From bottom to top: $\delta = 0, 0.25, 0.5, 1$ ($J = 0.5$, $g = 10$).

obtain

$$m_z = \lim_{N \rightarrow \infty} \sqrt{\frac{|E_{gs}|}{JN}} = \sqrt{1 - 2n}. \quad (88)$$

In Fig. 8 the density of magnetization as function of the annealing time, τ , is depicted. As one can see, even moderate dissipation essentially decreases the number of defects in the system.

Due to the symmetry of the problem with respect to $k \rightarrow -k$, and since for each k there is independent evolution, the probability of the whole system to remain in the ground state at the end of evolution is the product

$$P_{gs} = \prod_{k>0} P_k^{gs}(\tau). \quad (89)$$

In the long wavelength approximation one can take into account only $\varphi_k = \pi/N$, and estimate P_{gs} as

$$P_{gs} \approx \frac{1 - e^{-2\pi\Re\nu}}{1 - e^{-2\pi\Re\nu} + e^{-2\pi\Re\nu - \Re z^2(\tau)}}, \quad (90)$$

where $\Re z^2(\tau) = 2\delta J\tau/g^2$ and $\Re\nu = \tau/\tau_0$. Here we denote $\tau_0 = 2gN^2/(\pi^2 J)$.

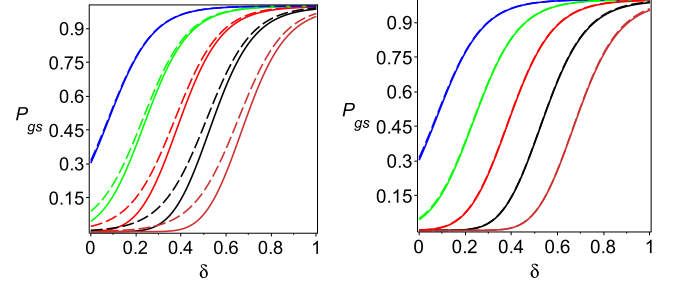


FIG. 9: (Color online) Probability to stay in the ground state, P_{gs} , as function of the dissipation parameter, δ ($J = 0.5$, $g = 10$, $\tau = 10^3$, $k = p - 1/2$). Left panel: Solid curves present the exact result. Dashed lines present the contribution of the first mode ($p = 1$). Right panel: Solid curves are the contribution of all modes. Dashed lines are the contribution of the first $p = 1, 2, \dots, N/64$ modes. From top to bottom: $N = 64, 128, 256, 512, 1024$.

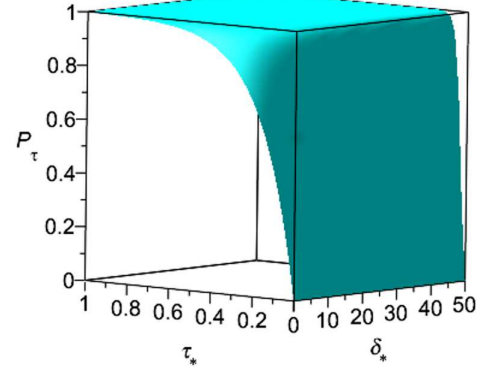


FIG. 10: (Color online) The transition probability, P_τ , as function of a scaled decay rate, $\delta_* = \delta\tau_0/g^2$, and scaled annealing time, $\tau_* = \tau/\tau_0$.

In Figs. 9 and 10, the results of numerical simulation are demonstrated. As one can see, for the probability $P_{gs} \approx 1$ the asymptotic formula of Eq. (90) is in a good agreement with the exact formula (89). We also performed numerical simulations to demonstrate that for any N the contribution of the first $N/64$ modes yields essentially the same result as the exact formula (89). (See Fig. 9.) We find that even moderate dissipation boosts the transition probability.

For the Hermitian QA ($\delta = 0$), Eq. (90) yields the Landau-Zener formula [28, 29]

$$P_{gs} = 1 - e^{-2\pi\tau/\tau_0}. \quad (91)$$

From here it follows that $P_{gs} \approx 1$, if $\tau \geq \tau_0$. Thus, the computational time for the Hermitian QA should be of order N^2 .

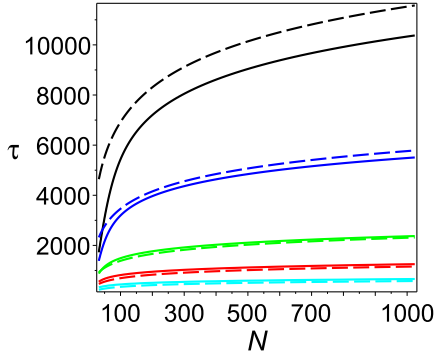


FIG. 11: (Color online) Annealing time, τ , as a function of N for NQA ($J = 0.5$, $g = 10$). Solid lines present the exact result. Dashed lines are the asymptotic formula of Eq.(96). From top to bottom: $\delta = 0.05, 0.1, 0.25, 0.5, 1$.

For the NQA, assuming $\tau \ll \tau_0$, we obtain

$$P_{gs} \approx \frac{1}{1 + \frac{\tau_0}{2\pi\tau} e^{-2J\delta\tau/g^2}}. \quad (92)$$

From here, in the limit of $\delta \rightarrow 0$, we obtain

$$P_{gs} \rightarrow \frac{1}{1 + \frac{\tau_0}{2\pi\tau}} \ll 1. \quad (93)$$

The obtained result is expected, as in this case, the time of the Hermitian annealing, τ , is small with respect to the characteristic time, τ_0 : $\tau \ll \tau_0$.

Next, assuming

$$\frac{2J\delta\tau}{g^2} - \ln \frac{\tau_0}{2\pi\tau} \gg 1. \quad (94)$$

we obtain

$$P_{gs} \approx 1 - \frac{\tau_0}{2\pi\tau} e^{-2J\delta\tau/g^2}. \quad (95)$$

As one can see, $P_{gs} \approx 1$, if the conditions of Eq. (94) are satisfied. From (94) we obtain the following rough estimate of the computational time for NQA: $\tau \approx (g^2/2J\delta) \ln N$.

To find the annealing time from the exact formula (90) we impose the following condition on the probability: $P_\tau = 0.999$. Then, we solved numerically Eq. (90). The results of numerical calculations are presented in Fig. 11. We find that the best fit of the asymptotic expression to the exact result is given by the following asymptotic formula (see Fig. 11):

$$\tau \approx \frac{g^2}{2J\delta} \ln \frac{N}{\pi}. \quad (96)$$

In Fig. 12, the annealing time, τ , as a function of the number of spins is depicted for NQA (left panel) and Hermitian QA (right panel). The comparison shows that

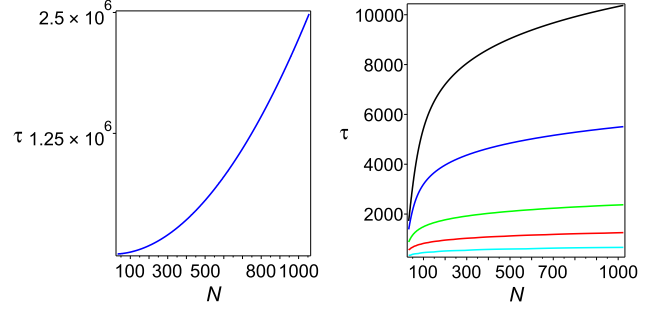


FIG. 12: (Color online) Annealing time, τ , as function of N . Left panel. Hermitian QA, $\delta = 0$ ($J = 0.5$, $g = 10$). Right panel. Non-Hermitian QA, from top to bottom: $\delta = 0.05, 0.1, 0.25, 0.5, 1$.

for large number of spins ($N \sim 1000$) and for $\delta \gtrsim 0.25$, the annealing time of NQA is $\approx 10^3$ times smaller than for Hermitian QA.

The obtained results indicate that the characteristic time of non-Hermitian annealing, even for small but finite $\delta \neq 0$, is defined not only by the number of spins, N (as in Hermitian annealing), but mainly by the dissipation rate, δ . (See Figs. 9, 10 and Eq. (92).) Thus, the non-Hermitian quantum annealing has complexity of order $\ln N$, which is much better than the quantum Hermitian (global) adiabatic algorithm. Also, this complexity is certainly better than one of the adiabatic local annealing algorithm which has a total running time of order N [43].

VI. CONCLUSION

Recently, many modifications of quantum annealing algorithms have been proposed [1–6, 8–10, 44, 45]. The main objective of these publications is to significantly decrease the time of annealing, so that the solutions of hard optimization problems could be obtained either by (i) combining classical computers with quantum algorithms or by (ii) building real quantum computers. One of the very popular test models is the Ising spin system which is also useful for practical purposes. In this case, the quantum annealing algorithms are used to find the ground state of this system.

In this paper we explored efficiency of NQA algorithm on a conventional computer, in application to the ferromagnetic Ising spin chain. We have chosen an auxiliary Hamiltonian in such a way that the total Hamiltonian is non-Hermitian. This allowed us to shift the minimal gap in the energy spectrum in the complex plane in the region of short wave excitations, and significantly reduce the time required to find the ground state.

Our approach leads to the annealing time $\sim \ln N$, where N is the number of spins, which is much less than the time of Hermitian annealing ($\sim N^2$) for the same problem. But many serious problems still remain to be considered. One of them is the application of this dissi-

pative approach to more complicated Ising-type models with frustrated interactions and to large-size systems. To overcome the problem of large-size systems, one may apply the density matrix renormalization group technique to carry out quantum annealing by real-time evolution for large systems [3, 48]. Another direction is to use both dissipation and pumping into the system, as it was done in [49, 50]. This research is now in progress.

Acknowledgments

The work by G.P.B. was carried out under the auspices of the National Nuclear Security Administration of the U.S. Department of Energy at Los Alamos National Laboratory under Contract No. DE-AC52-06NA25396. A.I.N. acknowledges the support from the CONACyT, Grant No. 118930. J.C.B.Z. acknowledges the support from the CONACyT, Grant No. 171014.

Appendix A: Exact solution of the Non-Hermitian Landau-Zener problem

The non-Hermitian Hamiltonian, $\mathcal{H}_k(t)$, projected on the two-dimensional subspace spanned by $|k_1\rangle = \begin{pmatrix} 1 \\ 0 \end{pmatrix}$ and $|k_0\rangle = \begin{pmatrix} 0 \\ 1 \end{pmatrix}$, takes the form

$$\mathcal{H}_k(t) = -\varepsilon_0(t)\mathbb{I} + J \begin{pmatrix} \tilde{g}(t) - \cos \varphi_k & \sin \varphi_k \\ \sin \varphi_k & -\tilde{g}(t) + \cos \varphi_k \end{pmatrix} \quad (\text{A1})$$

where $\varepsilon_0(t) = J \cos \varphi_k + iJ\delta(t)$ and $\tilde{g}(t) = g(t) + i\delta(t)$. We assume a linear dependence of the function, $\tilde{g}(t)$, on time:

$$\tilde{g}(t) = \begin{cases} \gamma(\tau - t), & 0 \leq t \leq \tau \\ 0, & t > \tau \end{cases}, \quad (\text{A2})$$

where, $\gamma = (g + i\delta)/\tau$, and g, δ are real parameters.

The general wave functions, $|\psi_k\rangle$ and $\langle\tilde{\psi}_k|$, satisfy the Schrödinger equation and its adjoint equation

$$i \frac{\partial}{\partial t} |\psi_k\rangle = \mathcal{H}_k(t) |\psi_k\rangle, \quad (\text{A3})$$

$$-i \frac{\partial}{\partial t} \langle\tilde{\psi}_k| = \langle\tilde{\psi}_k| \mathcal{H}_k(t). \quad (\text{A4})$$

Presenting $|\psi_k(t)\rangle$ as a linear superposition

$$|\psi_k(t)\rangle = (u_k(t)|k_0\rangle + v_k(t)|k_1\rangle) e^{i \int \varepsilon_0(t) dt}, \quad (\text{A5})$$

and inserting (A5) into Eq. (A3), we obtain

$$i\dot{u}_k = J(-(\tilde{g} - \cos \varphi_k) u_k + \sin \varphi_k v_k), \quad (\text{A6})$$

$$i\dot{v}_k = J(\sin \varphi_k u_k + (\tilde{g} - \cos \varphi_k) v_k). \quad (\text{A7})$$

Let $z_k(t) = e^{i\pi/4} \sqrt{2J/\gamma} (\gamma(\tau - t) - \cos \varphi_k)$ be a new variable. Then, for new functions, $u_k(t) = U_k(z_k)$ and

$v_k(t) = V_k(z_k)$, we write Eqs. (A6), (A7) in the standard Landau-Zener form [28, 29]

$$\frac{d}{dz_k} U_k = -\frac{z_k}{2} U_k + \sqrt{i\nu_k} V_k, \quad (\text{A8})$$

$$\frac{d}{dz_k} V_k = \frac{z_k}{2} V_k + \sqrt{i\nu_k} U_k, \quad (\text{A9})$$

where $\nu_k = J \sin^2 \varphi_k / 2\gamma$, and the complex ‘time’ z_k runs from $z_k(0) = e^{i\pi/4} \sqrt{2J/\gamma} (\gamma\tau - \cos \varphi_k)$ to $z_k(\tau) = -e^{i\pi/4} \sqrt{2J/\gamma} \cos \varphi_k$.

From Eqs. (A8), (A9) we obtain the second order Weber equation

$$\frac{d^2}{dz_k^2} U_k + \left(\frac{1}{2} - \frac{z_k^2}{4} - i\nu_k \right) U_k = 0, \quad (\text{A10})$$

$$\frac{d^2}{dz_k^2} V_k - \left(\frac{1}{2} + \frac{z_k^2}{4} + i\nu_k \right) V_k = 0. \quad (\text{A11})$$

Solution of the Weber’s equation is given by the parabolic cylinder functions $D_{-i\nu_k}(\pm z)$, $D_{i\nu_k-1}(\pm iz)$.

We obtain the solutions of Eqs. (A8, A9) in the form

$$U_k(z_k) = B_k D_{-i\nu_k}(z_k) - i\sqrt{i\nu_k} A_k D_{i\nu_k-1}(iz_k), \quad (\text{A12})$$

$$V_k(z_k) = A_k D_{i\nu_k}(iz_k) - \sqrt{i\nu_k} B_k D_{-i\nu_k-1}(z_k), \quad (\text{A13})$$

where the constants, A_k and B_k , are determined from the initial conditions.

If the evolution of TLS starts at $t_0 = 0$ in the ‘ground’ state, $|\psi(0)\rangle = |k_0\rangle$, the following initial conditions should be imposed: $u_k(0) = 1$ and $v_k(0) = 0$. Using the identity (A43), we obtain

$$A_k = \sqrt{i\nu_k} e^{\pi\nu_k/2} D_{-i\nu_k-1}(z_k(0)), \quad (\text{A14})$$

$$B_k = e^{\pi\nu_k/2} D_{i\nu_k}(iz_k(0)). \quad (\text{A15})$$

We assume further that $\tau \gg g/J$. This implies $|z_k(0)| \gg 1$. Then, applying the asymptotic formulas for the parabolic cylinder functions with $-3\pi/4 < \arg z_k < 3\pi/4$, we obtain

$$A_k = 0 + \mathcal{O}(1/|z_k(0)|), \quad (\text{A16})$$

$$B_k = (z_k(0))^{i\nu_k} e^{z_k^2(0)/4}. \quad (\text{A17})$$

Similar consideration of the adjoint Schrödinger equation with the wavefunction

$$\langle\tilde{\psi}_k| = (\tilde{u}_k(t)\langle k_0| + \tilde{v}_k(t)\langle k_1|) e^{-i \int \varepsilon_0(t) dt}, \quad (\text{A18})$$

yields

$$i\dot{\tilde{u}}_k = -J(-(\tilde{g} - \cos \varphi_k) \tilde{u}_k + \sin \varphi_k \tilde{v}_k), \quad (\text{A19})$$

$$i\dot{\tilde{v}}_k = -J(\sin \varphi_k \tilde{u}_k + (\tilde{g} - \cos \varphi_k) \tilde{v}_k). \quad (\text{A20})$$

For the functions, $\tilde{u}_k(t) = \tilde{U}_k(z_k)$ and $\tilde{v}_k(t) = \tilde{V}_k(z_k)$, we obtain

$$\frac{d}{dz_k} \tilde{U}_k = \frac{z_k}{2} \tilde{U}_k - \sqrt{i\nu_k} \tilde{V}_k, \quad (\text{A21})$$

$$\frac{d}{dz_k} \tilde{V}_k = -\frac{z_k}{2} \tilde{V}_k - \sqrt{i\nu_k} \tilde{U}_k. \quad (\text{A22})$$

From here it follows

$$\frac{d^2}{dz_k^2} \tilde{U}_k - \left(\frac{1}{2} + \frac{z_k^2}{4} + i\nu_k \right) \tilde{U}_k = 0, \quad (\text{A23})$$

$$\frac{d^2}{dz_k^2} \tilde{V}_k + \left(\frac{1}{2} - \frac{z_k^2}{4} - i\nu_k \right) \tilde{V}_k = 0. \quad (\text{A24})$$

The solutions are given by

$$\tilde{U}_k(z_k) = \tilde{A}_k D_{-i\nu_k-1}(z_k) + \tilde{B}_k D_{i\nu_k}(iz_k), \quad (\text{A25})$$

$$\tilde{V}_k(z_k) = \frac{1}{\sqrt{i\nu_k}} \tilde{A}_k D_{-i\nu_k}(z_k) + i\sqrt{i\nu_k} \tilde{B}_k D_{i\nu_k-1}(iz_k), \quad (\text{A26})$$

where

$$\tilde{A}_k = \nu_k e^{\pi\nu_k/2} D_{i\nu_k-1}(iz_k(0)), \quad (\text{A27})$$

$$\tilde{B}_k = e^{\pi\nu_k/2} D_{-i\nu_k}(z_k(0)). \quad (\text{A28})$$

For $|z_k(0)| \gg 1$ we obtain

$$\tilde{A}_k = 0 + \mathcal{O}(1/|z_k(0)|), \quad (\text{A29})$$

$$\tilde{B}_k = e^{\pi\nu_k/2} (z_k(0))^{-i\nu_k} e^{-z_k^2(0)/4}. \quad (\text{A30})$$

Finally, the straightforward computation shows that the obtained solutions satisfy the normalization condition $\langle \tilde{\psi}_k(t) | \psi_k(t) \rangle = 1$.

The solutions of the Schrödinger equations for $|z_k(0)| \gg 1$ and the initial conditions: $u_k(0) = \tilde{u}_k(0) = 1$, $v_k(0) = \tilde{v}_k(0) = 0$, are given by

$$U_k(z_k) = B_k D_{-i\nu_k}(z_k), \quad (\text{A31})$$

$$V_k(z_k) = -\sqrt{i\nu_k} B_k D_{-i\nu_k-1}(z_k), \quad (\text{A32})$$

$$\tilde{U}_k(z_k) = \tilde{B}_k D_{i\nu_k}(iz_k), \quad (\text{A33})$$

$$\tilde{V}_k(z_k) = i\sqrt{i\nu_k} \tilde{B}_k D_{i\nu_k-1}(iz_k), \quad (\text{A34})$$

where

$$B_k = (z_k(0))^{i\nu_k} e^{z_k^2(0)/4}, \quad (\text{A35})$$

$$\tilde{B}_k = e^{\pi\nu_k/2} (z_k(0))^{-i\nu_k} e^{-z_k^2(0)/4}. \quad (\text{A36})$$

1. Some important properties of the Weber functions

The parabolic cylinder functions, $D_{-i\nu_k}(\pm z)$, $D_{i\nu_k-1}(\pm iz)$, being solution of the linear differential equation

$$\frac{d^2 U}{dz^2} + \left(\frac{1}{2} + \nu - \frac{z^2}{4} \right) U = 0, \quad (\text{A37})$$

satisfy the following derivative and recurrence relations [41]:

$$\frac{d}{dz_k} \left(e^{z_k^2/4} D_{-i\nu_k}(z_k) \right) = i\nu_k e^{z_k^2/4} D_{-i\nu_k-1}(z_k), \quad (\text{A38})$$

$$\frac{d}{dz_k} \left(e^{-z_k^2/4} D_{-i\nu_k}(z_k) \right) = -e^{-z_k^2/4} D_{-i\nu_k+1}(z_k). \quad (\text{A39})$$

$$D_{-i\nu_k+1}(z_k) - z_k D_{-i\nu_k}(z_k) + \nu_k D_{-i\nu_k-1}(z_k) = 0. \quad (\text{A40})$$

The Wronskian for these solutions is given by

$$D_{-i\nu_k}(z_k) \frac{d}{dz_k} D_{-i\nu_k}(-z_k) - D_{-i\nu_k}(-z_k) \frac{d}{dz_k} D_{-i\nu_k}(z_k) = \frac{\sqrt{2\pi}}{\Gamma(i\nu_k)}, \quad (\text{A41})$$

$$D_{-i\nu_k}(z_k) \frac{d}{dz_k} D_{i\nu_k+1}(iz_k) - D_{i\nu_k+1}(iz_k) \frac{d}{dz_k} D_{-i\nu_k}(z_k) = -ie^{\pi\nu_k/2}. \quad (\text{A42})$$

Using Eqs. (A38) – (A42), we obtain

$$D_{-i\nu_k}(z_k) D_{i\nu_k}(iz_k) + \nu_k D_{-i\nu_k-1}(z_k) D_{i\nu_k-1}(iz_k) = e^{-\pi\nu_k/2} \quad (\text{A43})$$

For small value of the argument one can use the power-series expansion of Weber function yielding

$$D_{-i\nu_k}(z_k) = 2^{-i\nu_k/2} \frac{\sqrt{\pi}}{\Gamma\left(\frac{1}{2} + \frac{i\nu_k}{2}\right)}, \quad \text{as } |z_k| \rightarrow 0. \quad (\text{A44})$$

a. Asymptotic expansion for large value of argument

For large value of argument, $|z_k| \gg 1$, and for $|\arg z_k| < 3\pi/4$ the following asymptotic expansion is valid [41]

$$D_{-i\nu_k}(z_k) = z_k^{-i\nu_k} e^{-z_k^2/4} (1 + \mathcal{O}(|z_k^2|^{-1})) \quad (\text{A45})$$

To find the asymptotics of the Weber functions for other values of its argument one can use the relations:

$$D_{-i\nu_k}(z_k) = e^{-\pi\nu_k} D_{-i\nu_k}(-z_k) - \frac{i\sqrt{2\pi}}{\Gamma(i\nu_k)} e^{-\pi\nu_k/2} D_{i\nu_k-1}(iz_k). \quad (\text{A46})$$

In particular, for $-5\pi/4 < \arg z_k < -\pi/4$, this yields

$$D_{-i\nu_k}(z_k) = z_k^{-i\nu_k} e^{-z_k^2/4} (1 + \mathcal{O}(|z_k^2|^{-1})) + \frac{i\sqrt{2\pi}}{\Gamma(i\nu_k)} e^{-\pi\nu_k} z_k^{i\nu_k-1} e^{z_k^2/4} (1 + \mathcal{O}(|z_k^2|^{-1})). \quad (\text{A47})$$

b. Large-order asymptotics

For large-order value of the Weber functions with a phase of argument $|\arg z_k| < \pi/2$ the leading terms are [46, 47]

$$D_{-i\nu_k}(z_k) \sim \cos \frac{\theta_k}{2} e^{\pi\nu_k/4 - i\eta} \left(1 + \mathcal{O}\left(\frac{1}{\sqrt{|\nu_k|}}\right) \right), \quad (\text{A48})$$

$$D_{-i\nu_k-1}(z_k) \sim \frac{1}{\sqrt{i\nu_k}} \sin \frac{\theta_k}{2} e^{\pi\nu_k/4 - i\eta} \left(1 + \mathcal{O}\left(\frac{1}{\sqrt{|\nu_k|}}\right) \right), \quad (\text{A49})$$

where

$$\eta = -\frac{\nu_k}{2} + \nu_k \ln \left(\frac{1}{2} \left(z_k e^{-i\pi/4} + \sqrt{4\nu_k^2 - iz_k^2} \right) \right) + \frac{z_k e^{-i\pi/4}}{4} \sqrt{4\nu_k^2 - iz_k^2}, \quad (\text{A50})$$

and

$$\cos \theta_k = \frac{z_k}{\sqrt{z_k^2 + 4i\nu_k^2}}. \quad (\text{A51})$$

Appendix B: Equation of motion

We consider a two-level system governed by the non-Hermitian Hamiltonian, $\tilde{\mathcal{H}}_{\text{eff}}$, written as

$$\tilde{\mathcal{H}}_{\text{eff}} = \frac{\tilde{\lambda}_0}{2} \mathbf{1} + \frac{1}{2} \tilde{\mathbf{\Omega}}(t) \cdot \boldsymbol{\sigma}, \quad (\text{B1})$$

where $\tilde{\mathbf{\Omega}}(t) = (\tilde{\Omega}_x(t), \tilde{\Omega}_y(t), \tilde{\Omega}_z(t))$ is the complex vector and $\tilde{\lambda}_0 = \lambda_0 - i\Gamma$, where $\Gamma = (\Gamma_0 + \Gamma_1)/2$. The qubit states $|u(t)\rangle$ and $\langle u(t)|$ satisfy the Schrödinger equation:

$$i \frac{\partial |u(t)\rangle}{\partial t} = \tilde{\mathcal{H}}_{\text{eff}} |u(t)\rangle, \quad (\text{B2})$$

$$-i \frac{\partial \langle u(t)|}{\partial t} = \langle u(t)| \tilde{\mathcal{H}}_{\text{eff}}^\dagger. \quad (\text{B3})$$

Employing Eqs.(B2), (B3), we find that the Bloch vector, $\mathbf{n}(t) = \langle u(t)|\boldsymbol{\sigma}|u(t)\rangle$, satisfies the following generalized Bloch equation:

$$\frac{d\mathbf{n}}{dt} = -\Gamma \mathbf{n} + n \Im \tilde{\mathbf{\Omega}}(t) + \Re \tilde{\mathbf{\Omega}}(t) \times \mathbf{n}, \quad (\text{B4})$$

$$\frac{dn}{dt} = -\Gamma n + \Im \tilde{\mathbf{\Omega}}(t) \cdot \mathbf{n}, \quad (\text{B5})$$

where $n = \sqrt{n_x^2 + n_y^2 + n_z^2}$. Denoting the real part of the complex vector $\tilde{\mathbf{\Omega}} = \mathbf{\Omega} + i\boldsymbol{\Lambda}$ as $\Re \tilde{\mathbf{\Omega}} = (\Omega_x, \Omega_y, \Omega_z)$ and

its imaginary part as $\Im \mathbf{\Omega} = (\Lambda_x, \Lambda_y, \Lambda_z)$, we obtain

$$\frac{dn_x}{dt} = -\Gamma n_x + \Lambda_x n + \Omega_y n_z - \Omega_z n_y, \quad (\text{B6})$$

$$\frac{dn_y}{dt} = -\Gamma n_y + \Lambda_y n - \Omega_x n_z + \Omega_z n_x, \quad (\text{B7})$$

$$\frac{dn_z}{dt} = -\Gamma n_z + \Lambda_z n + \Omega_x n_y - \Omega_y n_x, \quad (\text{B8})$$

$$\frac{dn}{dt} = -\Gamma n + \Lambda_x n_x + \Lambda_y n_y + \Lambda_z n_z. \quad (\text{B9})$$

In terms of the Bloch vector the qubit state population of upper/lower level can be written as follows

$$\rho_{11}(t) = \frac{1}{2}(n(t) + n_z(t)), \quad (\text{B10})$$

$$\rho_{00}(t) = \frac{1}{2}(n(t) - n_z(t)). \quad (\text{B11})$$

This yields, $n_z(t) = \rho_{11}(t) - \rho_{00}(t)$ and $n(t) = \rho_{11}(t) + \rho_{00}(t)$. Substituting these expressions for $n_z(t)$ and $n(t)$ into Eqs. (B6) - (B9), we obtain

$$\begin{aligned} \frac{dn_x}{dt} = & -\Gamma n_x + \Lambda_x(\rho_{11} + \rho_{00}) \\ & + \Omega_y(\rho_{11} - \rho_{00}) - \Omega_z n_y, \end{aligned} \quad (\text{B12})$$

$$\begin{aligned} \frac{dn_y}{dt} = & -\Gamma n_y + \Lambda_y(\rho_{11} + \rho_{00}) \\ & - \Omega_x(\rho_{11} - \rho_{00}) + \Omega_z n_x, \end{aligned} \quad (\text{B13})$$

$$\begin{aligned} \frac{d\rho_{11}}{dt} = & -(\Gamma - \Lambda_z)\rho_{11} + \frac{1}{2}(\Lambda_x n_x + \Lambda_y n_y) \\ & + \frac{1}{2}(\Omega_x n_y - \Omega_y n_x), \end{aligned} \quad (\text{B14})$$

$$\begin{aligned} \frac{d\rho_{00}}{dt} = & -(\Gamma + \Lambda_z)\rho_{00} + \frac{1}{2}(\Lambda_x n_x + \Lambda_y n_y) \\ & - \frac{1}{2}(\Omega_x n_y - \Omega_y n_x), \end{aligned} \quad (\text{B15})$$

$$\frac{dn}{dt} = -\Gamma n + \Lambda_x n_x + \Lambda_y n_y + \Lambda_z(\rho_{11} - \rho_{00}). \quad (\text{B16})$$

-
- [1] T. Kadowaki and H. Nishimori, Phys. Rev. E **58**, 5355 (1998).
 - [2] E. Farhi, J. Goldstone, S. Gutmann, J. Lapan, A. Lundgren, and D. Preda, Science **292**, 472 (2001).
 - [3] S. Suzuki and M. Okada, in *Quantum Annealing and Related Optimization Methods*, edited by A. Das and B. K. Chakrabarti (Springer, 2005), vol. 679 of *Lecture Notes in Physics*, pp. 207 – 238.
 - [4] A. Das and B. K. Chakrabarti, Rev. Mod. Phys. **80**, 1061 (2008).
 - [5] G. E. Santoro, R. Martonak, E. Tosatti, and R. Car, Science **295**, 2427 (2002).
 - [6] M. Ohzeki and H. Nishimori, J. Comp. Theor. Nanoscience **8**, 963 (2011).
 - [7] S. Tanaka and R. Tamura, in *Lectures on Quantum Com-*

- puting, Thermodynamics and Statistical Physics*, edited by M. Nakahara and S. Tanaka (World Scientific, 2012), vol. 8 of *Kinki University Series on Quantum Computing*, pp. 3–62.
- [8] L. Stella, G. E. Santoro, and E. Tosatti, Phys. Rev. B **72**, 014303 (2005).
- [9] S. Suzuki, H. Nishimori, and M. Suzuki, Phys. Rev. E **75**, 051112 (2007).
- [10] M. H. S. Amin, Phys. Rev. Lett. **100**, 130503 (2008).
- [11] V. N. Smelyanskiy, U. v Toussaint, and D. A. Timucin, *Dynamics of quantum adiabatic evolution algorithm for Number Partitioning*, arXiv: quant-ph/0202155.
- [12] T. Jörg, F. Krzakala, J. Kurchan, and A. C. Maggs, Phys. Rev. Lett. **101**, 147204 (2008).
- [13] A. P. Young, S. Knysh, and V. N. Smelyanskiy, Phys.

- Rev. Lett. **101**, 170503 (2008).
- [14] G. P. Berman and A. I. Nesterov, IJQI **7**, 1469 (2009).
 - [15] A. I. Nesterov and G. P. Berman, Phys. Rev. A **86**, 052316 (2012).
 - [16] M. V. Berry, Proc. R. Soc. A **392**, 45 (1984).
 - [17] M. V. Berry and M. Wilkinson, Proc. Roy. Soc. A **392**, 15 (1984).
 - [18] P. M. Morse and H. Feshbach, *Methods of Theoretical Physics* (McGraw-Hill, New York, 1953).
 - [19] A. P. Seyranian, O. N. Kirillov and A. A. Mailybaev, J. Phys. A: Math. Gen. **38**, 1723 (2005).
 - [20] O. N. Kirillov, A. A. Mailybaev, and A. P. Seyranian, J. Phys. A **38**, 5531 (2005).
 - [21] A. A. Mailybaev, O. N. Kirillov, and A. P. Seyranian, Doklady Math. **73**, 129 (2006).
 - [22] S. Katsura, Phys. Rev. **127**, 1508 (1962).
 - [23] J. Dziarmaga, Phys. Rev. Lett. **95**, 245701 (2005).
 - [24] A. C. M. Carollo and J. K. Pachos, Phys. Rev. Lett. **95**, 157203 (2005).
 - [25] A. I. Nesterov and S. G. Ovchinnikov, Phys. Rev. E **78**, 015202(R) (2008).
 - [26] E. Lieb, T. Schultz, and D. Mattis, Ann. Phys. **16**, 407 (1961).
 - [27] M. N. Lebedev, *Special Functions & Their Applications* (Dover, New York, 1972).
 - [28] L. Landau and E. M. Lifshitz, *"Quantum Mechanics"* (Pergamon, New York, 1958).
 - [29] C. Zener, Proc. R. Soc. A **137**, 696 (1932).
 - [30] M. V. Berry, Proc. Roy. Soc. A **430**, 405 (1990).
 - [31] A. Joye, G. Mileti, and C.-E. Pfister, Phys. Rev. A **44**, 4280 (1991).
 - [32] H. K. A. Joye and C. E. Pfister, Ann. Phys. **208**, 299 (1991).
 - [33] A. Kvitsinsky and S. Putterman, J. Math. Phys. **32**, 1403 (1991).
 - [34] R. Schilling, M. Vogelsberger, and D. A. Garanin, J. Phys. A **39**, 13727 (2006).
 - [35] G. Dridi, S. Guérin, H. R. Jauslin, D. Viennot, and G. Jolicard, Phys. Rev. A **82**, 022109 (2010).
 - [36] A. M. Dykhne, Sov. Phys.-JETP **14**, 941 (1962).
 - [37] J. P. Davis and P. Pechukas, J. Chem. Phys. **64**, 3129 (1976).
 - [38] J.-T. Hwang and P. Pechukas, J. Chem. Phys. **67**, 4640 (1977).
 - [39] S. Suzuki and M. Okada, J. Phys. Soc. Japan **74**, 1649 (2005).
 - [40] T. Caneva, R. Fazio, and G. E. Santoro, Phys. Rev. B **76**, 144427 (2007).
 - [41] A. Erdélyi, W. Magnusand, and F. Oberhettinger, *Higher Transcendental Functions*, vol. I (McGraw-Hill, New York, 1953).
 - [42] W. H. Zurek, U. Dorner, and P. Zoller, Phys. Rev. Lett. **95**, 105701 (pages 4) (2005).
 - [43] J. Roland and N. J. Cerf, Phys. Rev. A **65**, 042308 (2002).
 - [44] M. Ohzeki, Phys. Rev. Lett. **105**, 050401 (2010).
 - [45] M. Ohzeki and H. Nishimori, Comp. Phys. Com. **182**, 257 (2011).
 - [46] F. W. J. Olver, J. Res. Natl. Bur. Stand. B **63**, 131 (1959).
 - [47] N. V. Vitanov and B. M. Garraway, Phys. Rev. A **53**, 4288 (1996).
 - [48] S. R. White and A. E. Feiguin, Phys. Rev. Lett. **93**, 076401 (2004).
 - [49] S. Utsunomiya, K. Takata, and Y. Yamamoto, Optics Express, **19**, 18091 (2011).
 - [50] K. Takata, S. Utsunomiya, and Y. Yamamoto, New J. Phys. **14**, 013052 (2012).
 - [51] Approximation $\cos \varphi_k \approx 1$ instead of $\cos \varphi_k \approx 1 - \varphi_k^2/2$ leads to omission of corrections to the formula (37) up to $\mathcal{O}(\delta/g)$.